$[Co_4O_4]^{4+}$ Cubane Core as a Brønsted Base: Preparation and Properties of $[Co_4O_3(OH)(O_2CR)_2(bpy)_2]^{3+}$ and $[Co_4O_2(OH)_2(O_2CR)_2(bpy)_2]^{4+}$ Salts

Katerina Dimitrou, Angelica D. Brown, Kirsten Folting, and George Christou*

Department of Chemistry and Molecular Structure Center, Indiana University, Bloomington, Indiana 47405-4001

Received October 21, 1998

The preparation and properties are described of complexes resulting from the mono- and diprotonation of the $[Co_4O_4]^{4+}$ unit to give products containing $[Co_4O_3(OH)]^{5+}$ and $[Co_4O_2(OH)_2]^{6+}$, respectively. Treatment of $[Co_4O_4(O_2CC_6H_4\text{-}p\text{-}OMe)_2(bpy)_4]^{2+}$ (bpy = 2,2′-bipyridine) in MeCN with 70% perchloric acid leads to isolation of $[Co_4O_2(OH)_2(O_2CC_6H_4\text{-}p\text{-}OMe)_2(bpy)_4](ClO_4)_4$ (**5**) in 61% yield. Treatment of $[Co_4O_4(O_2CC_6H_4\text{-}p\text{-}Me)_2(bpy)_4]^{2+}$ in MeCN with an acidic solution of $(NH_4)_3[Ce(NO_3)_6]$ leads to isolation of $[Co_4O_3(OH)(O_2CC_6H_4\text{-}p\text{-}Me)_2(bpy)_4][Ce(NO_3)_6]$ (**6**) in 96% yield. Complex **5**·3MeCN·H_2O crystallizes in monoclinic space group *C*2/*c* with (at −155 °C) $a = 33.838(8)$ Å, $b = 13.826(3)$ Å, $c = 29.944(7)$ Å, $\beta = 98.84(1)°$, and $Z = 8$. Complex **6**·PhCN·H_2O crystallizes in orthorhombic space group *Pbca* with (at −154 °C) $a = 22.603(4)$ Å, $b = 34.759(6)$ Å, $c = 18.167(3)$ Å, and $Z = 8$. The complexes contain $[Co_4O_2(OH)_2]^{6+}$ (**5**) and $[Co_4O_3(OH)]^{5+}$ (**6**) distorted-cubane cores, the sites of protonation being apparent by (i) the approach of ClO_4^- or $[Ce(NO_3)_6]^{3-}$ anions to within hydrogen-bonding distances (O···O ≈ 2.7 Å) and (ii) the longer Co−OH^- bond lengths compared with Co−O^{2-} bond lengths. Peripheral ligation is provided by chelating bpy and *syn*,*syn*-bridging RCO_2^- groups. The Co^{III} atoms are six-coordinate and approximately octahedral. Solution studies show that the diprotonated species is a strong diprotic acid analogous to H_2SO_4; the first deprotonation goes to completion, but the monoprotonated species is a weak acid and is in equilibirium with the nonprotonated species. pH studies in aqueous solution yield a pK_{a2} value of 3.15 for the second deprotonation. Electronic and ^1H NMR spectra of the diprotonated complexes in various solvents are consistent with the monoprotonated complex being the major species in solution. The combined results demonstrate that the $[Co_4O_4]^{4+}$ core is capable of acting as a Brønsted base, undergoing either one or two protonation reactions.

Introduction

In the last several years, we have developed a strong interest in 3d metal carboxylate chemistry, as it has become apparent that this area represents a rich source of high-nuclearity, oxide-bridged products with interesting structural, spectroscopic, and magnetic properties.[1−6] The majority of our efforts have been concentrated in Mn chemistry, and to a lesser extent in V, Fe, and Ni chemistry, but we recently also initiated studies in Co carboxylate chemistry. In recent reports, we have described how a variety of Co clusters could be obtained spanning nuclearities of 2−8 and involving Co^{III} or mixed-valence Co^{II}/Co^{III} oxidation levels. Such species have included $[Co_3O(OH)_3(O_2CMe)_2(bpy)_3](ClO_4)_2$,[7] $[Co_4O_4(O_2CMe)_2(bpy)_4](ClO_4)$,[7] $[Co_8O_4(O_2CPh)_{12}(MeCN)_3(H_2O)]$,[8] and $[Co_8O_4(OH)_4(O_2CMe)_6L_2](ClO_4)_2$,[9] where L is a bis-bipyridyl ligand.

The Co_4 complex contains a $[Co_4O_4]^{4+}$ cubane core, the first example of such a species (although additional examples have since been identified[10,11]), and this structural motif is also to be found in the Co_8 complexes. In $[Co_8O_4(O_2CPh)_{12}(MeCN)_3(H_2O)]$, the $[Co_4O_4]^{4+}$ cubane is acting as a quadruple bridge to four Co^{II} ions, the μ_3-O^{2-} ions of the cubane core thus becoming μ_4.[8] In $[Co_8O_4(OH)_4(O_2CMe)_6L_2]^{2+}$, the core consists of three face-fused $[Co_4O_4]^{4+}$ cubane units, the central one of which is $[Co_4O_4]^{4+}$ and the end faces being $[Co_2(OH)_2]$ containing Co^{II} ions.[9] Since in both Co_8 complexes the $[Co_4O_4]^{4+}O^{2-}$ ions thus retain sufficient basicity to bind to a Lewis-acidic Co^{II} ion, it was suspected that the $[Co_4O_4]^{4+}$ might also be capable of undergoing protonation reactions under fairly mild conditions. This has proved to be the case, and this paper describes the preparation and characterization of mono- and diprotonated derivatives of the $[Co_4O_4]^{4+}$ core. Portions of this work have been briefly communicated.[12]

(1) Aromi, G.; Aubin, S. M. J.; Bolcar, M. A.; Christou, G.; Eppley, H. J.; Folting, K.; Hendrickson, D. N.; Huffman, J. C.; Squite, R. C.; Tsai, H.-L.; Wang, S.; Wemple, M. W. *Polyhedron* **1998**, *17*, 3005.
(2) Karet, G.; Sun, Z.; Heinrich, D. D.; McKusker, J. K.; Folting, K.; Streib, W. E.; Huffman, J. C.; Hendrickson, D. N.; Christou, G. *Inorg. Chem.* **1996**, *35*, 6450.
(3) Castro, S. L.; Sun, Z.; Grant, C. M.; Bollinger, J. C.; Hendrickson, D. N.; Christou, G. *J. Am. Chem. Soc.* **1998**, *120*, 2365.
(4) Grant, C. M.; Knapp, M. J.; Huffman, J. C.; Hendrickson, D. N.; Christou, G. *Chem. Commun.* **1998**, 1753.
(5) Halcrow, M. A.; Sun, J.-S.; Huffman, J. C.; Christou, G. *Inorg. Chem.* **1995**, *34*, 4167.
(6) Christou, G. In *Magnetism: A Supramolecular Function*; Kahn, O., Ed.; NATO ASI Series; Kluwer: Dordrecht, 1996.
(7) Dimitrou, K.; Folting, K.; Streib, W. E.; Christou G. *J. Am. Chem. Soc.* **1993**, *115*, 6432.
(8) Dimitrou, K.; Chen, S.-J.; Folting, K.; Christou, G. *Inorg. Chem.* **1995**, *34*, 4160.
(9) Grillo, V. A.; Sun, Z.; Folting, K.; Hendrickson, D. N.; Christou, G. *J. Chem. Soc., Chem. Commun.* **1996**, 2233.
(10) Ama, T.; Okamoto, K.; Yonemura, T.; Kawaguchi, H.; Takeuchi, A.; Yasui, T. *Chem. Lett.* **1997**, 1189.
(11) Beattie, J. K.; Hambley, T. W.; Klepetko, J. A.; Masters, A. F.; Turner, P. *Polyhedron* **1998**, *17*, 1343.
(12) Dimitrou, K.; Folting, K.; Streib, W. E.; Christou, G. *J. Chem. Soc., Chem. Commun.* **1994**, 1385.

10.1021/ic981237n CCC: $18.00
Published on Web 03/25/1999

Experimental Section

Syntheses. All manipulations were carried out under aerobic conditions unless otherwise noted. Reagent grade solvents were used without further purification. Ammonium cerium (IV) nitrate (Aldrich) and other common chemicals were used as received. $[Co_4O_4(O_2CC_6H_4$-*p*-Me$)_2$(bpy)$_4$](ClO$_4$)$_2$ (**1**) and $[Co_4O_4(O_2CC_6H_4$-*p*-OMe$)_2$(bpy)$_4$](ClO$_4$)$_2$ (**2**) were available from previous work.[7,13] **CAUTION:** Complexes containing perchlorate ions are potentially explosive. Handling of only small quantities and the use of appropriate caution are advised.

$[Co_4O_2(OH)_2(O_2CC_6H_4$-*p*-Me$)_2(bpy)_4$]Cl$_4$ (3). A solution of complex **1**·H$_2$O (0.29 g, 0.21 mmol) in MeCN (25 mL) was slowly treated with HCl (1.0 mL, 35%) in MeCN (4 mL) with stirring, and a color change from brown to greenish-brown was observed, followed by the formation of a black precipitate. The reaction mixture was stirred for a further 10 min, the solution becoming almost colorless, and the black microcrystalline precipitate was collected by filtration, washed with MeCN (4 mL) and copious amounts of THF, and dried under vacuum for 2 days. The yield was 90% (0.27 g). Anal. Calcd for $Co_4O_{14}C_{56}H_{60}N_8Cl_4$ (**3**·6H$_2$O): C, 46.49; H, 4.18; N, 7.75; Cl, 9.80. Found: C, 46.50; H, 4.15; N, 7.78; Cl, 9.90. IR data (cm^{-1}) (KBr pellet): 3407 (m, br), 3075 (w), 3035 (w), 1606 (m), 1584 (w), 1516 (m), 1502 (m), 1472 (m), 1448 (s), 1402 (vs), 1318 (w), 1308 (w), 1246 (w), 1180 (m), 1157 (w), 1107 (w), 1039 (w), 1020 (w), 768 (s), 728 (m), 668 (w), 654 (m), 640 (w), 615 (w), 589 (m), 578 (m), 479 (w), 467 (w).

$[Co_4O_2(OH)_2(O_2CC_6H_4$-*p*-Me$)_2(bpy)_4$](ClO$_4$)$_4$ (4). A solution of complex **1**·H$_2$O (0.10 g, 0.14 mmol) in MeCN (25 mL) was slowly treated with HClO$_4$ (2 mL, 70%) with stirring, and a color change from brown to greenish-brown was observed, followed by the formation of a black precipitate. The reaction mixture was stirred for a further 10 min, and the flask was stored at −15 °C overnight. The black microcrystalline precipitate was collected by filtration, washed with MeCN (4 mL) and copious amounts of THF, and dried under vacuum overnight. The yield was 67% (0.08 g). Anal. Calcd for $Co_4O_{27.5}C_{56}H_{55}N_8Cl_4$ (**4**·3$^1/_2$H$_2$O): C, 40.58; H, 3.34; N, 6.76; Cl, 8.56. Found: C, 40.47; H, 3.38; N, 6.76; Cl, 8.60. The acetate complex $[Co_4O_2(OH)_2(O_2CMe)_2$(bpy)$_4$](ClO$_4$)$_4$ can be made in a similar fashion.

$[Co_4O_2(OH)_2(O_2CC_6H_4$-*p*-OMe$)_2(bpy)_4$](ClO$_4$)$_4$ (5). A solution of complex **2** (0.20 g, 0.14 mmol) in MeCN (30 mL) was slowly treated with HClO$_4$ (3 mL, 70%) with stirring, and a color change from brown to greenish-brown was observed. After 5 min, Et$_2$O (90 mL) was added, and the flask was stored in the freezer overnight to produce a crystalline solid. This was collected by filtration, washed with THF and Et$_2$O, and dried under vacuum overnight. The yield was 61% (0.14 g). Anal. Calcd for $Co_4O_{30}C_{56}H_{56}N_8Cl_4$ (**5**·4H$_2$O): C, 39.60; H, 3.32; N, 6.60; Cl, 8.35. Found: C, 39.64; H, 3.33; N, 6.61; Cl, 8.44.

$[Co_4O_3(OH)(O_2CC_6H_4$-*p*-Me$)_2$(bpy)$_4$][Ce(NO$_3$)$_6$] (6). Method A. A solution of $(NH_4)_2[Ce(NO_3)_6]$ (0.55 g, 1.00 mmol) and NH_4NO_3 (0.10 g, 1.25 mmol) in H$_2$O (30 mL) was treated with H$_2$O$_2$ (5 mL, 50%), and the reaction mixture was boiled. The initial yellow solution slowly became colorless. After 2 h, the concentrated solution (2 mL) was cooled to room temperature and added to a solution of complex **1**·H$_2$O (0.21 g, 0.15 mmol) in MeCN (30 mL) to give a dark olive green precipitate, the mother liquor becoming almost colorless. After 15 min, complex **6** was isolated by filtration, washed with copious amounts of MeCN, and dried under vacuum. The yield was 96% (0.25 g). Anal. Calcd for $Co_4CeO_{28}C_{56}H_{50}N_{14}$ (**6**·2H$_2$O): C, 38.57; H, 2.95; N, 11.24. Found: C, 38.47; H, 2.89; N, 11.21.

Method B. A solution of complex **1**·H$_2$O (0.035 g, 0.025 mmol) in PhCN/EtOH (7/10 mL) was layered with a solution of $(NH_4)_2[Ce(NO_3)_6]$ (0.02 g, 0.04 mmol) in EtOH. After two weeks, large black crystals were formed, and a sample for crystallography was kept in contact with the mother liquor. The bulk crystals were collected by filtration, washed with EtOH, and dried under vacuum. The yield was 90% (0.04 g).

X-ray Crystallography. Data were collected on a Picker four-circle diffractometer at ca. −155 °C; details of the diffractometry, low-temperature facilities, and computational procedures employed by the Molecular Structure Center are available elsewhere.[14] Unit cell parameters are listed in Table 1. Black crystals of **5**·3MeCN·H$_2$O and **6**·PhCN·H$_2$O of suitable size (0.10 × 0.24 × 0.45 mm and 0.28 × 0.26 × 0.26 mm, respectively) were affixed to glass fibers using silicone grease and then transferred to goniostats and cooled to ca. −155 °C for characterization and data collection.

Table 1. Crystallographic Data for Complexes **5**·3MeCN·H$_2$O and **6**·PhCN·H$_2$O

	5	**6**
formula[a]	$C_{62}H_{59}N_{11}O_{27}Cl_4Co_4$	$C_{63}H_{54}N_{15}O_{27}Co_4Ce$
fw, g/mol	1767.75	1829.06
space group	*C*2/*c*	*Pbca*
a, Å	33.838(8)	22.603(4)
b, Å	13.826(3)	34.759(6)
c, Å	29.944(7)	18.167(3)
β, deg	98.84(1)	90
V, Å^3	13842	14273
Z	8	8
T, °C	−155	−154
radiation, Å	0.710 69	0.710 69
ρ_{calc}, g/cm^3	1.697	1.702
μ, cm^{-1}	11.825	16.344
obsd data ($F > 3\sigma(F)$)	5083	4249
R (R_w), %	5.59 (5.72)	8.63 (8.78)

[a] Including solvate molecules. [b] Graphite monochromator. [c] $R = 100\sum(|F_o| - |F_c|)/\sum|F_o|$. [d] $R_w = 100\ [\sum w(|F_o| - |F_c|)^2/\sum w|F_o|^2]^{1/2}$, where $w = 1/\sigma^2(|F_o|)$.

For **5**·3MeCN·H$_2$O, a systematic search of selected regions of reciprocal space yielded a set of reflections that exhibited monoclinic diffraction symmetry (2/*m*). The systematic extinction of *hkl* for $h + k = 2n + 1$, *h*0*l* for $h = 2n + 1$, and $l = 2n + 1$ identified the possible space groups as *C*2/*c* or *Cc*. The choice of the centrosymmetric space group *C*2/*c* was confirmed by the subsequent successful solution and refinement of the structure. A total of 11 095 reflections (including standards) was collected ($+h$, $+k$, $\pm l$; $6° \le \theta \le 45°$) and data processing gave a unique set of 9089 reflections and a residual of 0.075 for the averaging of 1169 reflections measured more than once. Plots of four standard reflections measured every 300 reflections showed no significant trends. No absorption correction was performed. The initial stages of the structure solution were carried out using the full data set. The crystal structure was solved using SHELXS-86, and most of the atoms of the cation and the four anions were located in the initial solution. The remaining atoms were located in several iterations of least-squares refinement and difference Fourier map calculation. Several hydrogen atoms were located in a later difference map, notably H(1) and H(2) on O(7) and O(8). The full-matrix least-squares refinement was completed using anisotropic thermal parameters on the atoms of the cation and anions, isotropic thermal parameters on solvent atoms, and fixed, idealized hydrogen atoms on the cation, with the exception of H(1) and H(2), which were refined using isotropic thermal parameters. The final $R(F)$ was 0.056 using 5083 reflections considered observed by the criterion $F > 3.0\sigma(F)$. For the full data set, the $R(F)$ was 0.083. The total number of variables was 952, and the refinement was carried out in a cyclic fashion owing to the large number of variables. Atoms O(7) and O(8) are hydrogen-bonded to oxygen atoms O(82) and O(85) in two of the anions. The asymmetric unit also contains solvent molecules: there are three MeCN molecules, two of which are disordered (one badly, modeled as a cluster of C atoms), and a H$_2$O molecule with partial occupancy (25%); the formulation **5**·3MeCN·H$_2$O was assumed for calculations of formula weight, density, etc. The final difference map was essentially featureless, the largest peak being 0.67 e/Å^3 near a C atom of the badly disordered MeCN molecule. Final R (R_w) values are listed in Table 1.

For **6**·PhCN·H$_2$O, a selective search of a limited hemisphere of reciprocal space revealed a primitive orthorhombic cell. Following complete intensity data collection ($+h$, $+k$, $+l$; $6° \le \theta \le 45°$), the conditions $k = 2n$ for 0*k*1, $l = 2n$ for *h*01, and $h = 2n$ for *hk*0 uniquely

(13) Dimitrou, K.; Brown, A. D.; Streib, W. E.; Christou, G. Manuscript in preparation.

(14) Chisholm, M. H.; Folting, K.; Huffman, J. C.; Kirkpatrick, C. C. *Inorg. Chem.* **1984**, *23*, 1021.

Scheme 1

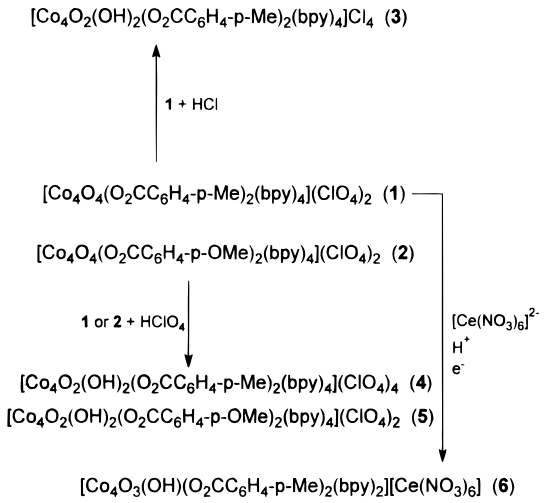

determined the space group as *Pbca*. Data processing gave a residual of 0.041 for the averaging of 1241 unique intensities that had been observed more than once. Four standard reflections measured every 400 reflections showed no significant trends. No correction was made for absorption. The structure was solved using a combination of direct methods (MULTAN78) and Fourier techniques. The positions of the Ce and Co atoms were obtained from an initial E-map, and the positions of the remaining non-hydrogen atoms were obtained from subsequent iterations of least-squares refinement and difference Fourier map calculation. There is a large amount of disorder in the $[Ce(NO_3)_6]^{3-}$ anion, and the 18 oxygen atoms were modeled as 12 full-weight atoms and 12 half-weight atoms. In addition, one of the toluate ligands is undergoing some disorder resulting in large thermal parameters and rather poor distances and angles for that group. There are also solvent molecules present but only at partial occupancy: a molecule of C_6H_5CN refined to an occupancy of about 1/2 and the oxygen atom of a water molecule refined to an occupancy of about 2/3. These occupancies were then fixed for the final refinement cycles. Only a few of the hydrogen atoms were observed; hydrogen atoms bonded to carbon atoms were included in fixed, calculated positions with appropriate weights and with thermal parameters fixed at one plus the thermal parameter of the atom to which they were bonded. In the final cycles of refinement, the non-hydrogen atoms in the cation and Ce(77) were varied with anisotropic thermal parameters, and the remaining non-hydrogen atoms involving the disordered anion and the solvent were varied with isotropic thermal parameters. The final $R(F)$ was 0.086 for the 851 variables refined using 4249 data with $F > 3\sigma(F)$. The largest peak in the final difference map was 2.8 e/Å^3 located 1.3 Å from Ce(77) in the disordered anion. Final R (R_w) values are listed in Table 1.

Results

Syntheses. The transformations to be described are summarized for convenience in Scheme 1. Initial protonation experiments were carried out using $[Co_4O_4(O_2CC_6H_4\text{-}p\text{-}Me)_2(bpy)_4](ClO_4)_2$ (**1**) and concentrated (35%) aqueous hydrochloric acid. Acidification of stirred MeCN solutions of **1** gave a noticeable color change from brown to greenish-brown, followed by formation of a black microcrystalline precipitate in 90% yield. Elemental analysis of vacuum-dried material was consistent with the formulation $[Co_4O_2(OH)_2(O_2CC_6H_4\text{-}p\text{-}Me)_2(bpy)_4]Cl_4$ (**3**), the double-protonation being suggested by the Cl analysis fitting a Co:Cl ratio of 1:1. Confirmation of the doubly protonated nature of the product was sought by X-ray crystallography, and suitable crystals were grown by diffusive mixing of MeCN solutions of **1** and aqueous HCl. The crystal structure of **3**·2MeCN·8H_2O showed two Cl^- ions within hydrogen-bonding distance of two $[Co_4O_4]$ core oxygen atoms ($Cl\cdots O = 2.972(15)$ and 2.924(15) Å), suggesting these oxygen atoms to be protonated (i.e., OH^- ions) and the core to be $[Co_4O_2(OH)_2]^{6+}$. Unfortunately, only one other Cl^- ion was unambiguously identified with 100% occupancy in the lattice, the fourth expected Cl^- being disordered between two positions, each with 50% occupancy; it was recognized that such partial-occupancy Cl^- ions could not be unambiguously distinguished from H_2O groups, and notwithstanding the high Cl elemental analysis, it was concluded that unequivocal confirmation of a $[Co_4O_2(OH)_2(O_2CR)_2(bpy)_4]^{4+}$ tetracation would require preparation of a salt with a more securely identifiable anion.

The use of an MeCN solution of concentrated (70%) perchloric acid for protonation of **1** proceeded analogously, giving a black precipitate of **4** in 67% yield. Large crystals could be grown from unstirred solutions maintained at room temperature, but these were found to be poor diffractors of X-rays. Thus, the carboxylate group was varied, and use of the *p*-methoxybenzoate (anisate) complex **2** gave the corresponding complex **5**, which was more soluble in MeCN and required addition of Et_2O for crystallization: black crystals grown from an MeCN/Et_2O layering were found suitable for crystallographic studies, and the latter (vide infra) provided unequivocal confirmation of the formula of **5** to be $[Co_4O_2(OH)_2(O_2CC_6H_4\text{-}p\text{-}OMe)_2(bpy)_4](ClO_4)_4$ and, by implication, that of **3** to be $[Co_4O_2(OH)_2(O_2CC_6H_4\text{-}p\text{-}Me)_2(bpy)_4]Cl_4$. The double-protonation reaction is summarized by eq 1. The protonated complexes

$$[Co_4O_4(O_2CR)_2(bpy)_4]^{2+} + 2H^+ \rightarrow [Co_4O_2(OH)_2(O_2CR)_2(bpy)_4]^{4+} \quad (1)$$

3−**5** are stable in air once isolated, although it should be noted that prolonged contact of **3** (24 h) with the highly acidic mother liquor caused conversion of the black crystalline solid to a green oil, with the appearance of colorless crystals, probably bipyridinium chloride(s). Crystals of **3** and **5** growing slowly in layerings were therefore isolated and washed as soon as they were judged large enough for crystallographic studies.

A monoprotonated complex was also prepared. After preliminary experimentation, two procedures were developed, both employing the trianionic $[Ce(NO_3)_6]^{3-}$ ion to favor precipitation of the tricationic (i.e., monoprotonated) $[Co_4O_3(OH)(O_2CR)_2(bpy)_4]^{3+}$ ion from solutions likely containing $[Co_4O_4]^{4+}$, $[Co_4O_3(OH)]^{5+}$, and $[Co_4O_2(OH)_2]^{6+}$ species in equilibrium. Thus, addition of acidic $[Ce(NO_3)_6]^{3-}$ solutions, generated *in situ* by reduction of $[Ce(NO_3)_6]^{2-}$ with H_2O_2, were added to MeCN solutions of **1** to rapidly precipitate sparingly soluble $[Co_4O_3(OH)(O_2CC_6H_4\text{-}p\text{-}Me)_2(bpy)_4][Ce(NO_3)_6]$ (**6**) in essentially quantitative yield (96%). An alternative method, which also gave single crystals suitable for X-ray crystallography, involved diffusive mixing of **1** and $[Ce(NO_3)_6]^{2-}$ solutions in PhCN/EtOH and EtOH, respectively; the Ce^{IV} is slowly reduced under these conditions, giving slow formation of **6**. Both methods can be summarized by the general eq 2; note that no mineral acid was employed, the preparations taking advantage of the inherent acidity of $[Ce(NO_3)_6]^{z+}$ solutions.

$$[Co_4O_4(O_2CR)_2(bpy)_4]^{2+} + [Ce(NO_3)_6]^{2-} \xrightarrow[+\,H^+]{+\,e^-} [Co_4O_3(OH)(O_2CR)_2(bpy)_4][Ce(NO_3)_6] \quad (2)$$

Description of Structures. Labeled ORTEP plots of the cation of **5** and the cation/anion pair of **6** are shown in Figures 1 and 2, respectively; the former includes two of the four ClO_4^-

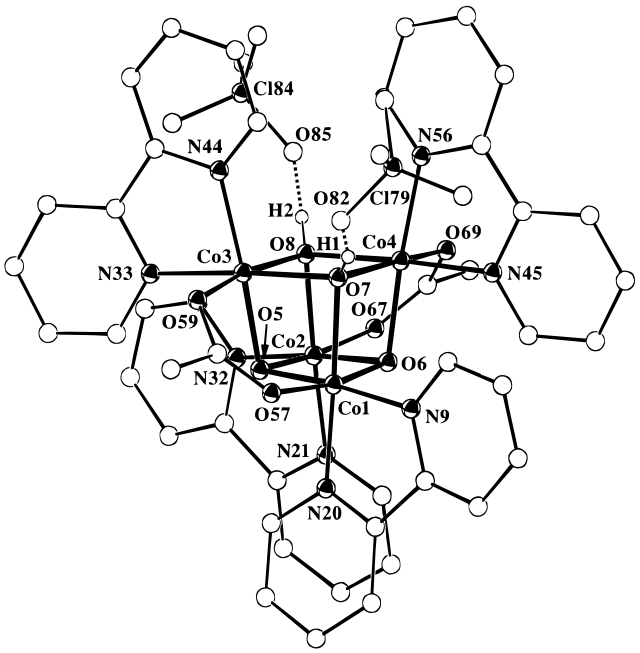

Figure 1. ORTEP representation at the 50% probability level of the $[Co_4O_2(OH)_2(O_2CC_6H_4\text{-}p\text{-}OMe)_2(bpy)_4]^{4+}$ cation of complex **5** and the two ClO_4^- anions hydrogen-bonded (dashed lines) to the OH^- groups. For clarity, only one carbon atom of each *p*-methylbenzoate group is shown.

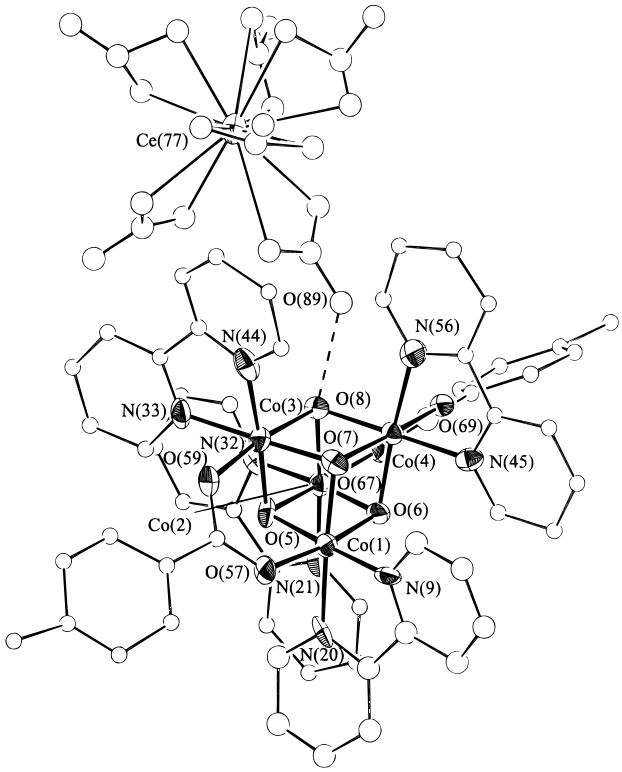

Figure 2. ORTEP representation at the 50% probability level of $[Co_4O_3(OH)(O_2CC_6H_4\text{-}p\text{-}Me)_2(bpy)_4][Ce(NO_3)_6]$ showing the hydrogen bond (dashed line) between the anion and the OH^- group.

anions. Selected interatomic distances and angles are listed in Tables 2 and 3. Complex **5**·3MeCN·H_2O crystallizes in monoclinic space group *C*2/*c*, with the asymmetric unit containing an entire cation, four ClO_4^- anions, and solvent molecules. The structure of the cation consists of a central $[Co_4O_2(OH)_2]^{6+}$ distorted cubane core; each Co^{III} is in a distorted octahedral environment, and peripheral ligation is provided by a chelating bpy on each metal and two carboxylate groups each bridging a Co_2 pair in their familiar *syn*,*syn* manner. Core oxygen atoms O(7) and O(8) are protonated as evidenced by (i) the close approach of two ClO_4^- anions to hydrogen-bonding distances (O(7)···O(82) = 2.69(1), O(8)···O(85) = 2.71(1) Å), and (ii) the longer Co−O bonds to O(7) and O(8) (1.944(6)−1.975(6); average 1.961 Å) than to O(5) and O(6) (1.857(6)−1.913(6); average 1.879 Å). The latter property causes a large distortion of the $[Co_4O_4]$ core, with the Co(3)···Co(4) separation, which is bridged by the two OH^- groups, being noticeably longer (3.060(2) Å) than the other Co···Co separations (2.748(2)−2.930(2) Å). The core consequently has virtual C_{2v} symmetry and the anion C_2 symmetry, the C_2 axis passing through the midpoint of, and perpendicular to, the Co(3)−O(7)−O(8)−Co(4) plane.

Complex **6**·PhCN·H_2O crystallizes in monoclinic space group *Pbca*, with the asymmetric unit containing a complete cation/

Table 2. Selected Interatomic Distances (Å) and Angles (deg) for Complex **5**

Co(1)−Co(2)	2.859(2)	Co(2)−N(21)	1.903(8)
Co(1)−Co(3)	2.748(2)	Co(2)−N(32)	1.951(8)
Co(1)−Co(4)	2.930(2)	Co(3)−O(5)	1.871(6)
Co(2)−Co(3)	2.912(2)	Co(3)−O(7)	1.975(6)
Co(2)−Co(4)	2.753(2)	Co(3)−O(8)	1.959(6)
Co(3)−Co(4)	3.060(2)	Co(3)−O(59)	1.881(6)
Co(1)−O(5)	1.861(6)	Co(3)−N(33)	1.916(7)
Co(1)−O(6)	1.913(6)	Co(3)−N(44)	1.953(7)
Co(1)−O(7)	1.958(6)	Co(4)−O(6)	1.874(6)
Co(1)−O(57)	1.912(6)	Co(4)−O(7)	1.958(6)
Co(1)−N(9)	1.960(7)	Co(4)−O(8)	1.973(6)
Co(1)−N(20)	1.913(7)	Co(4)−O(69)	1.885(6)
Co(2)−O(5)	1.898(6)	Co(4)−N(45)	1.910(7)
Co(2)−O(6)	1.857(6)	Co(4)−N(56)	1.975(7)
Co(2)−O(8)	1.944(6)	O(7)−O(82)	2.69(1)
Co(2)−O(67)	1.910(6)	O(8)−O(85)	2.71(1)

O(5)−Co(1)−O(6)	80.79(25)	O(6)−Co(1)−O(7)	80.18(25)
O(5)−Co(1)−O(7)	86.22(26)	O(6)−Co(1)−O(57)	171.07(26)
O(5)−Co(1)−O(57)	93.39(26)	O(6)−Co(1)−N(9)	99.32(27)
O(5)−Co(1)−N(9)	175.1(3)	O(6)−Co(1)−N(20)	100.7(3)
O(5)−Co(1)−N(20)	92.3(3)	O(7)−Co(1)−O(57)	92.75(25)
O(7)−Co(1)−N(9)	98.7(3)	O(5)−Co(3)−N(33)	91.8(3)
O(7)−Co(1)−N(20)	178.1(3)	O(5)−Co(3)−N(44)	173.8(3)
O(57)−Co(1)−N(9)	87.1(3)	O(7)−Co(3)−O(8)	77.77(25)
O(57)−Co(1)−N(20)	86.2(3)	O(7)−Co(3)−O(59)	92.63(25)
N(9)−Co(1)−N(20)	82.8(3)	O(7)−Co(3)−N(33)	177.0(3)
O(5)−Co(2)−O(6)	81.26(25)	O(7)−Co(3)−N(44)	99.9(3)
O(5)−Co(2)−O(8)	80.81(26)	O(8)−Co(3)−O(59)	169.39(27)
O(5)−Co(2)−O(67)	171.12(26)	O(8)−Co(3)−N(33)	102.9(3)
O(5)−Co(2)−N(21)	99.9(3)	O(8)−Co(3)−N(44)	97.0(3)
O(5)−Co(2)−N(32)	98.6(3)	O(59)−Co(3)−N(33)	86.4(3)
O(6)−Co(2)−O(8)	86.10(26)	O(59)−Co(3)−N(44)	89.07(28)
O(6)−Co(2)−O(67)	93.51(26)	N(33)−Co(3)−N(44)	82.9(3)
O(6)−Co(21)−N(21)	91.8(3)	O(6)−Co(4)−O(7)	81.16(25)
O(6)−Co(2)−N(32)	174.7(3)	O(6)−Co(4)−O(8)	84.83(25)
O(8)−Co(2)−O(67)	91.72(25)	O(6)−Co(4)−O(69)	94.12(25)
O(8)−Co(2)−N(21)	177.6(3)	O(6)−Co(4)−N(45)	92.1(3)
O(8)−Co(2)−N(32)	99.1(3)	O(6)−Co(4)−N(56)	174.0(3)
O(67)−Co(2)−N(21)	87.4(3)	O(7)−Co(4)−O(8)	77.85(25)
O(67)−Co(2)−N(32)	87.3(3)	O(7)−Co(4)−O(69)	169.30(27)
N(21)−Co(2)−N(32)	83.0(3)	O(7)−Co(4)−N(45)	102.0(3)
O(5)−Co(3)−O(7)	85.44(25)	O(7)−Co(4)−N(56)	97.55(28)
O(5)−Co(3)−O(8)	81.09(26)	O(8)−Co(4)−O(69)	92.22(26)
O(5)−Co(3)−O(59)	93.76(26)	O(8)−Co(4)−N(45)	176.9(3)
O(8)−Co(4)−N(56)	100.71(28)	Co(1)−O(6)−Co(4)	101.4(3)
O(69)−Co(4)−N(45)	87.7(3)	Co(2)−O(6)−Co(4)	95.11(26)
O(69)−Co(4)−N(56)	88.1(3)	Co(1)−O(7)−Co(3)	88.63(25)
N(45)−Co(4)−N(56)	82.4(3)	Co(1)−O(7)−Co(4)	96.86(27)
Co(1)−O(5)−Co(2)	99.01(27)	Co(3)−O(7)−Co(4)	102.14(28)
Co(1)−O(5)−Co(3)	94.85(27)	Co(2)−O(8)−Co(3)	96.54(27)
Co(2)−O(5)−Co(3)	101.2(3)	Co(2)−O(8)−Co(4)	89.33(27)
Co(1)−O(6)−Co(2)	98.61(26)	Co(3)−O(8)−Co(4)	102.2(3)

Table 3. Selected Interatomic Distances (Å) and Angles (deg) for Complex **6**

Ce(77)−O(78)	2.59(3)	Co(1)−O(57)	1.939(12)
Ce(77)−O(80)	2.40(6)	Co(1)−N(9)	1.901(20)
Ce(77)−O(82)	2.72(3)	Co(1)−N(20)	1.924(17)
Ce(77)−O(84)	2.74(3)	Co(2)−O(5)	1.882(13)
Ce(77)−O(86)	2.634(19)	Co(2)−O(6)	1.862(14)
Ce(77)−O(88)	2.750(16)	Co(2)−O(8)	1.939(12)
Ce(77)−O(90)	2.594(25)	Co(2)−O(67)	1.941(13)
Ce(77)−O(92)	2.65(4)	Co(2)−N(21)	1.902(17)
Ce(77)−O(94)	2.717(24)	Co(2)−N(32)	1.940(17)
Ce(77)−O(96)	2.78(5)	Co(3)−O(5)	1.871(13)
Ce(77)−O(98)	2.595(22)	Co(3)−O(7)	1.877(14)
Ce(77)−O(100)	2.571(23)	Co(3)−O(8)	1.932(12)
Co(1)−Co(3)	2.675(4)	Co(3)−O(59)	1.890(14)
Co(1)−Co(2)	2.870(4)	Co(3)−N(33)	1.964(17)
Co(1)−Co(4)	2.844(4)	Co(3)−N(44)	1.908(19)
Co(2)−Co(3)	2.888(4)	Co(4)−O(6)	1.868(13)
Co(2)−Co(4)	2.710(4)	Co(4)−O(7)	1.881(13)
Co(3)−Co(4)	2.933(4)	Co(4)−O(8)	1.929(13)
Co(1)−O(5)	1.897(13)	Co(4)−O(69)	1.967(13)
Co(1)−O(6)	1.893(13)	Co(4)−N(45)	1.924(17)
Co(1)−O(7)	1.871(13)	Co(4)−N(56)	1.964(18)
O(8)−O(89)	2.72(1)		

O(5)−Co(1)−O(6)	80.1(6)	O(6)−Co(2)−O(67)	93.1(6)
O(5)−Co(1)−O(7)	86.3(6)	O(6)−Co(2)−N(21)	93.2(7)
O(5)−Co(1)−O(57)	93.1(6)	O(6)−Co(2)−N(32)	174.8(7)
O(5)−Co(1)−N(9)	177.9(6)	O(8)−Co(2)−O(67)	93.2(5)
O(5)−Co(1)−N(20)	97.9(7)	O(8)−Co(2)−N(21)	176.0(6)
O(6)−Co(1)−O(7)	81.2(5)	O(8)−Co(2)−N(32)	97.2(6)
O(6)−Co(1)−O(57)	172.6(6)	O(67)−Co(2)−N(21)	90.8(6)
O(6)−Co(1)−N(9)	97.9(6)	O(67)−Co(2)−N(32)	90.0(6)
O(6)−Co(1)−N(20)	99.2(6)	N(21)−Co(2)−N(32)	82.7(7)
O(7)−Co(1)−O(57)	95.5(6)	O(5)−Co(3)−O(7)	86.9(6)
O(7)−Co(1)−N(9)	92.6(7)	O(5)−Co(3)−O(8)	81.6(5)
O(7)−Co(1)−N(20)	175.8(7)	O(5)−Co(3)−O(59)	92.0(6)
O(57)−Co(1)−N(9)	88.7(6)	O(5)−Co(3)−N(33)	94.9(7)
O(57)−Co(1)−N(20)	84.6(6)	O(5)−Co(3)−N(44)	175.8(7)
N(9)−Co(1)−N(20)	83.1(7)	O(7)−Co(3)−O(8)	79.2(5)
O(5)−Co(2)−O(6)	81.3(6)	O(7)−Co(3)−O(59)	96.5(6)
O(5)−Co(2)−O(8)	81.2(5)	O(7)−Co(3)−N(33)	178.2(7)
O(5)−Co(2)−O(67)	172.3(6)	O(7)−Co(3)−N(44)	97.3(7)
O(5)−Co(2)−N(21)	94.8(6)	O(8)−Co(3)−O(59)	172.5(6)
O(5)−Co(2)−N(32)	95.9(6)	O(8)−Co(3)−N(33)	101.1(6)
O(6)−Co(2)−O(8)	86.8(6)	O(8)−Co(3)−N(44)	100.0(6)
O(59)−Co(3)−N(33)	83.4(6)	O(69)−Co(4)−N(45)	85.3(6)
O(59)−Co(3)−N(44)	86.6(7)	O(69)−Co(4)−N(56)	89.2(6)
N(33)−Co(3)−N(44)	80.9(8)	N(45)−Co(4)−N(56)	82.5(7)
O(6)−Co(4)−O(7)	81.6(5)	Co(1)−O(5)−Co(2)	98.8(6)
O(6)−Co(4)−O(8)	86.9(6)	Co(1)−O(5)−Co(3)	90.4(6)
O(6)−Co(4)−O(69)	93.2(6)	Co(2)−O(5)−Co(3)	100.6(6)
O(6)−Co(4)−N(45)	91.7(7)	Co(1)−O(6)−Co(2)	99.7(6)
O(6)−Co(4)−N(56)	173.4(7)	Co(1)−O(6)−Co(4)	98.3(6)
O(7)−Co(4)−O(8)	79.2(5)	Co(2)−O(6)−Co(4)	93.2(6)
O(7)−Co(4)−O(69)	170.4(6)	Co(1)−O(7)−Co(3)	91.1(6)
O(7)−Co(4)−N(45)	102.9(6)	Co(1)−O(7)−Co(4)	98.6(6)
O(7)−Co(4)−N(56)	96.9(6)	Co(3)−O(7)−Co(4)	102.6(6)
O(8)−Co(4)−O(69)	92.5(5)	Co(2)−O(8)−Co(3)	96.5(5)
O(8)−Co(4)−N(45)	177.3(6)	Co(2)−O(8)−Co(4)	89.0(5)
O(8)−Co(4)−N(56)	99.1(6)	Co(3)−O(8)−Co(4)	98.9(6)

anion pair and solvent molecules. The structure of the cation consists of a central $[Co_4O_3(OH)]^{5+}$ distorted cubane core; as for **5**, each Co^{III} is in a distorted octahedral environment, with peripheral ligation provided by a total of four chelating bpy and two bridging RCO_2^- groups. Only one core oxygen atom is protonated, namely O(8), and this is hydrogen-bonded to a nitrate oxygen atom, O(89), from the $[Ce(NO_3)_6]^{3-}$ anion (O(8)···O(89) = 2.72(1) Å). The conclusion that O(8) is a OH^- atom is supported by the distances within the core: as for **5**, Co−O(8) bonds are noticeably longer (1.929(13)−1.939(12) Å) than other Co−O bonds (1.862(14)−1.897(13) Å), the range overlapping by the 3σ criterion due to the large esd values for **6** but the difference being undoubtedly real. Similarly, Co···Co separations bridged by O(8) are slightly longer (average 2.844 Å) than the rest (average 2.796 Å). The combined data clearly point to **6** containing a monoprotonated core. The virtual symmetry of the core is now C_s, with the mirror plane passing through Co(1), O(7), O(8), and Co(2); the complete cation has C_1 symmetry.

Table 4. Comparison of Core Structural Parameters (Å) for Complexes **1**, **5**, and **6**

parameter	$[Co_4O_4]^{4+}$ (**1**)	$[Co_4O_3(OH)]^{5+}$ (**6**)	$[Co_4O_2(OH)_2]^{6+}$ (**5**)
Co1···Co2	2.850(2)	2.870(4)	2.859(2)
Co1···Co3	2.666(2)	2.675(4)	2.748(2)
Co1···Co4	2.849(2)	2.844(4)	2.930(2)
Co2···Co3	2.865(2)	2.888(4)	2.912(2)
Co2···Co4	2.663(2)	2.710(4)	2.753(2)
Co3···Co4	2.845(2)	2.933(4)	3.060(2)
Co1−O5	1.877(6)	1.897(13)	1.861(6)
Co2−O5	1.895(6)	1.882(13)	1.898(6)
Co3−O5	1.878(6)	1.871(13)	1.871(6)
Co1−O6	1.891(6)	1.893(13)	1.913(6)
Co2−O6	1.873(6)	1.862(14)	1.857(6)
Co4−O6	1.874(6)	1.868(13)	1.874(6)
Co2−O8	1.877(6)	1.939(12)[a]	1.944(6)[a]
Co3−O8	1.890(6)	1.932(12)[a]	1.959(6)[a]
Co4−O8	1.880(6)	1.929(13)[a]	1.973(6)[a]
Co1−O7	1.874(6)	1.871(13)	1.958(6)[a]
Co3−O7	1.863(5)	1.877(14)	1.975(6)[a]
Co4−O7	1.893(5)	1.881(13)	1.958(6)[a]
V cube (Å^3)	6.869	7.006	7.297

[a] Distances involving OH^- ions. The labeling scheme is

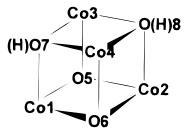

Comparison of the $[Co_4O_{4-x}(OH)_x]^{(4+x)+}$ (x = 0, 1, 2) Cores. The $[Co_4O_4]$ cubane core has now been structurally characterized at three different protonation levels (x = 0, 1, 2), and it is of interest to compare changes in structural parameters. In Table 4 are compared Co···Co and Co−O distances for complexes **1**, **5**, and **6**. Co···Co distances in **1** conform to the virtual D_{2d} core symmetry, with the S_4 axis passing through the opposite faces bridged by the two RCO_2^- groups (Figure 3); these faces contain noticeably shorter Co···Co separations (2.663(2), 2.666(2) Å) than the other faces (2.845(2)−2.865(2) Å). All Co−O distances are essentially the same (by the 3σ criterion), but very slight differences consistent with D_{2d} symmetry are nevertheless noticeable: Co−O distances parallel to the S_4 axis appear slightly longer (1.890(6)−1.895(6) Å; average 1.892 Å) than those perpendicular (1.863(5)−1.880(6) Å; average 1.875 Å). Double protonation to give the core of **5** causes one face to enlarge dramatically, as described earlier, and the virtual core symmetry to be C_{2v}, with the C_2 axis perpendicular to the S_4 axis of **1** (Figure 3). The Co−O distances separate into four types, consistent with C_{2v} symmetry, with the calculated averages giving the order $a \approx b \gg c \approx d$. Note that small differences in the *trans* influences of bpy vs RCO_2^- are evident, and more precise comparisons under C_{2v} symmetry are unwarranted (the core more closely approximates C_2). In essence, all Co−OH^- bond lengths are noticeably longer (>1.94 Å) than Co−O^{2-} bond lengths. The Co···Co separations show a related variation, and note that the two Co_2 pairs bridged by RCO_2 are still the shortest in the core (Co(1)···Co(3) and Co(2)···Co(4)).

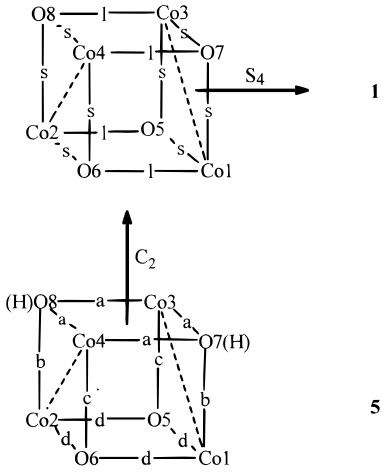

Figure 3. Cores of complexes **1** (top) and **5** (bottom) indicating the position of the S_4 and C_2 rotation axes; the dashed lines indicate the Co_2 pairs bridged by RCO_2^- groups. For **1**, *s* = short, *l* = long; for **5**, $a \approx b \gg c \approx d$. The labeling scheme for **5** in Figure 1 is employed for both drawings.

For complex **6**, the monoprotonation and resulting virtual C_s core symmetry lead to several types of Co−O distance, with the Co−OH^- distances being the longest (≥1.929(13) Å) and readily assignable. Co···Co separations again show a shortening of two *trans* Co···Co pairs bridged by RCO_2^- groups. The volumes of the three cores represent a convenient, single parameter with which to gauge the net effect of the protonations, and it can be seen that mono- and diprotonation cause increases of 0.137 and 0.428 Å^3, respectively, corresponding to approximately 2.0 and 6.2% increases compared with **1**.

Solution Studies. The acidic conditions required to generate the mono- and especially the diprotonated forms suggested that redissolution of the isolated $[Co_4O_2(OH)_2(O_2CR)_2(bpy)_4]^{4+}$ and $[Co_4O_3(OH)(O_2CR)_2(bpy)_4]^{3+}$ complexes should give fairly acidic solutions, and this was found to be the case. For example, a 5.00×10^{-3} M aqueous solution of complex **3** at 25 °C has a pH of 2.26 ± 0.01. A strong monoprotic acid such as $HClO_4$ would give a pH of 2.30 at this concentration. This indicates that the doubly protonated complexes are analogous to diprotic strong acids such as H_2SO_4, as summarized in eq 3; that is, the

$$[Co_4O_2(OH)_2]^{6+} \rightarrow [Co_4O_3(OH)]^{5+} + H^+ \overset{K_{a2}}{\rightleftharpoons} [Co_4O_4]^{4+} + H^+ \quad (3)$$

di- and monoprotonated forms are strong and weak acids, respectively. The low pH of the solutions is consistent with the first deprotonation occurring to completion, and this conclusion is also supported by the spectroscopic data described later (*vide infra*). To chararcterize the acid dissociation constant K_{a2} for the second deprotonation in eq 3, pH titrations with 0.1 M NaOH were carried out on 8.71×10^{-4} M aqueous solutions of $[Co_4O_2(OH)_2(O_2CMe)_2(bpy)_4](ClO_4)_4$. Multiple determinations gave a K_{a2} value of $7.1(8) \times 10^{-4}$. This corresponds to a pK_{a2} value of 3.15(5), making the monoprotonated cluster comparable in acid strength to 4-nitrobenzoic acid (3.41), iodoacetic acid (3.12), and chloroacetic acid (2.85). The predominant species in solutions of the mono- and diprotonated complexes is thus the monoprotonated form.

The electronic spectra of complex **3**, the most soluble of the diprotonated species, in various solvents reflect the presence of the transformations in eq 3; the spectra are slightly solvent- and concentration-dependent. The nonprotonated species such as **1** and **2** have a characteristic visible peak in the 410−420 nm range,[7,13] and this is shifted to higher energies for the protonated species, appearing as a shoulder in the 350−360 nm region in a variety of solvents, including H_2O, MeOH, and MeCN. The spectra for complex **5** and its nonprotonated version **2** in MeCN are compared in Figure 4. The spectra of diprotonated species in H_2O are essentially unchanged on addition of 1 equiv of NaOH, supporting the main species present in solutions of the diprotonated complex to be the monoprotonated complex. The solvent and concentration dependences are consistent with an equilibrium between mono- and nonprotonated species, with the former being the dominant species in solution.

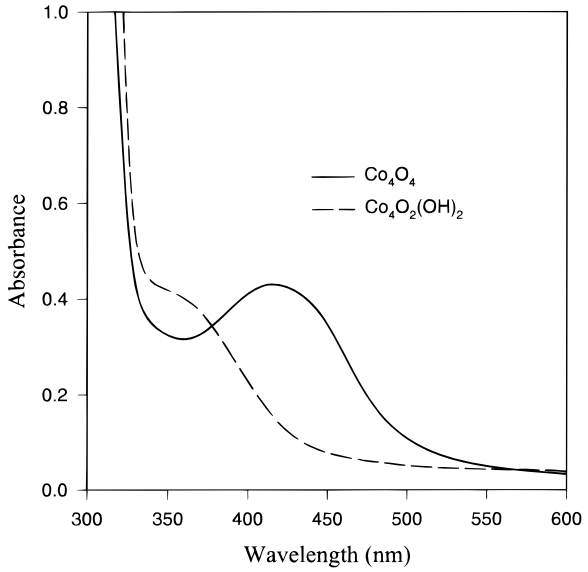

Figure 4. Electronic spectra of $[Co_4O_4(O_2CC_6H_4$-*p*-$Me)_2(bpy)_4](ClO_4)_2$ (**1**; solid line) and $[Co_4O_2(OH)_2(OH)_2(O_2CC_6H_4$-*p*-$Me)_2(bpy)_4](ClO_4)_4$ (**3**; dashed line) in MeCN.

Table 5. ^{1}H NMR Chemical Shift Data for Complexes **3** and **6**

complex	solvent	$\delta(RCO_2^-)$	δ(bpy)
3	CD_3CN	2.00 (s, 6H), 6.56 (d, 4H), 6.62 (d, 4H)	7.23 (t, 8H), 8.30 (t, 8H), 8.70 (d, 8H), 9.06 (8H)
	D_2O	1.85 (s, 6H), 6.35 (d, 4H), 6.50 (d, 4H)	7.19 (t, 8H), 8.22 (t, 8H), 8.42 (d, 8H), 8.64 (d, 8H)
	CD_3OH	2.02 (6H), 6.50 (4H), 6.58 (4H)	7.38 (8H), 8.41 (8H), 8.90 (16H)
	$(CD_3)_2SO$	1.94 (6H), 6.26 (4H), 6.57 (4H)	7.16 (8H), 8.30 (8H), 8.50 (8H), 8.95 (8H)
6	$(CD_3)_2SO$	1.93 (6H), 6.29 (4H), 6.58 (4H)	7.17 (8H), 8.32 (8H), 8.51 (8H), 8.97 (8H)

[a] ±0.02 ppm; approximately 5 mM concentrations.

As a further probe of the solution behavior, ^{1}H NMR spectra were recorded for complexes **3**−**6**. The diprotonated complexes all exhibit D_{2d} solution symmetry on the ^{1}H NMR time scale. The line widths of the resonances are dependent on the solvent employed, however, and representative data for complex **3** in four different solvents are presented in Table 5. Figure 5 shows the spectrum for **3** in CD_3CN and D_2O, together with the spectrum for the nonprotonated version **1** in CD_3CN for comparison. The spectrum of **3** in D_2O exhibits the narrowest peaks, and the resonances in CD_3CN are slightly broader. In CD_3OD, the resonances are all too broad to clearly show splitting from spin−spin coupling. These data indicate that exchange of H^+ between the four oxide ions in the $[Co_4O_4]$ core, and between the latter and free H_2O groups, is fast on the

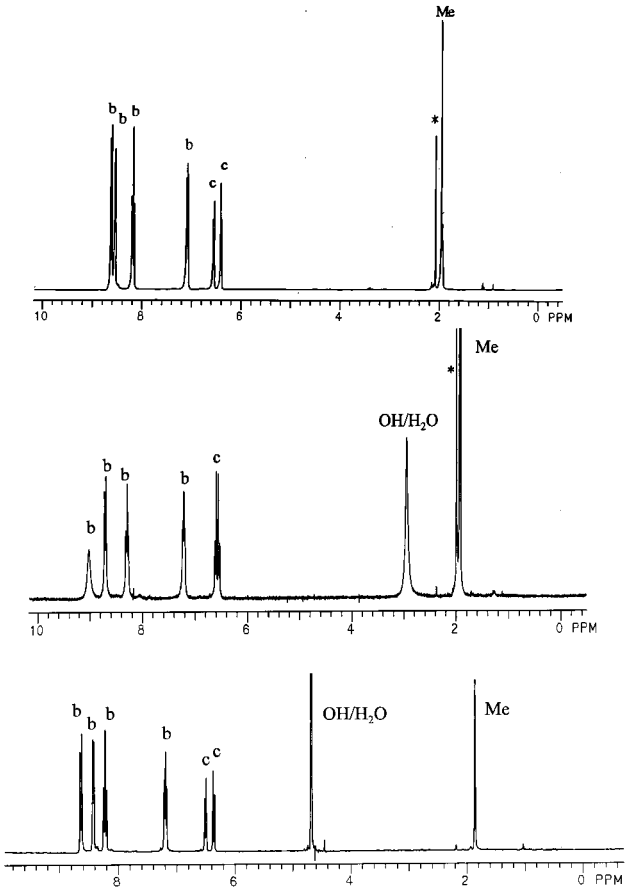

Figure 5. 300 MHz ^{1}H NMR spectra of $[Co_4O_4(O_2CC_6H_4$-*p*-Me$)_2$(bpy)$_4$](ClO$_4$)$_2$ (**1**) in CD_3CN (top), and $[Co_4O_2(OH)_2(O_2CC_6H_4$-*p*-Me$)_2(bpy)_4$]Cl$_4$ (**3**) in CD_3CN (middle) and D_2O (bottom): b = bpy, c = carboxylate, * = solvent impurities.

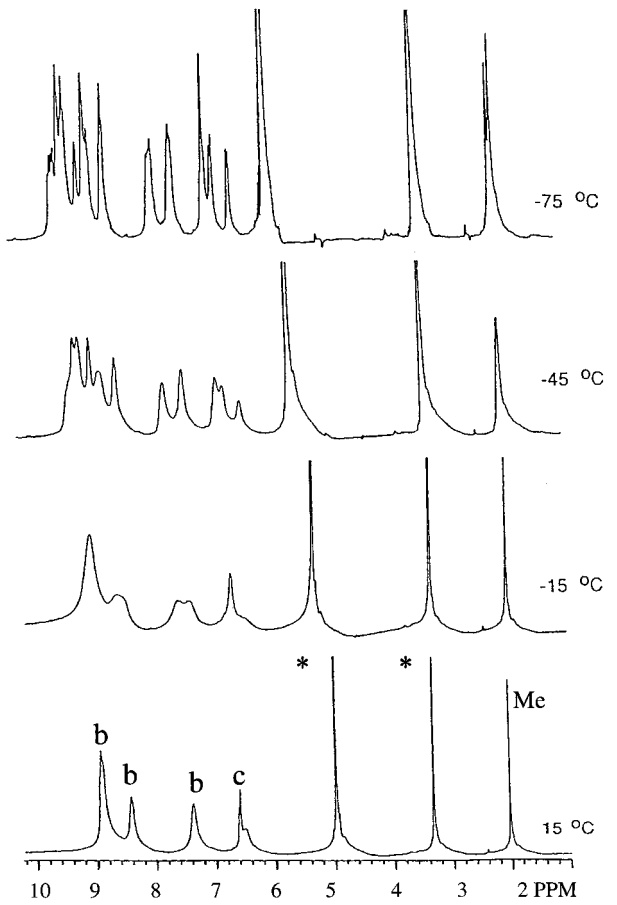

Figure 6. 300 MHz variable-temperature ^{1}H NMR spectra of $[Co_4O_2(OH)_2(O_2CC_6H_4$-*p*-Me$)_2(bpy)_4$]Cl$_4$ (**3**) in CD_3OD at the indicated temperatures: b = bpy, c = carboxylate, * = solvent impurities.

^{1}H NMR time scale, leading to effective D_{2d} symmetry for the cations in solution. The exact rate of this exchange would be expected to be solvent-dependent. The identity of the solvent will also influence the relative proportions of the species in the equilibrium of eq 3. In an attempt to slow the exchange rate, variable-temperature studies were performed on **3** in CD_3OD (Figure 6): as the temperature is lowered, the peaks broaden and then decoalesce to give a spectrum at −75 °C that contains many more bpy resonances than at 15 °C (>8, although the exact number is difficult to determine) and, more importantly, two *p*-Me resonances (of the toluate groups) at $\delta \approx 2$. This spectrum is consistent with the monoprotonated species, whose C_s symmetry (Figure 2) will give two *p*-Me signals and a maximum of 16 bpy signals if the H^+ is localized on one O^{2-} ion on the ^{1}H NMR time scale. The nonprotonated (D_{2d}) and diprotonated (C_2) (Figures 1 and 3) species are both expected to give a single *p*-Me resonance and only four bpy resonances and cannot thus be responsible for the observed spectrum at −75 °C. The VT behavior in Figure 6 thus provides additional support for the monoprotonated complex being the main species obtained on dissolution of the diprotonated complexes, with the effective D_{2d} symmetry at room temperature being due to fast H^+ exchange on the ^{1}H NMR time scale. The latter is also evident in the ^{13}C{^{1}H} NMR spectrum of **3** in CD_3OD, where only 10 resonances are observed, five from the bpy and five from the carboxylate groups. Solution studies on the monoprotonated complex **6** have been hampered by its low solubility: it is only significantly soluble in DMSO, and its ^{1}H NMR spectrum (Table 5) is broader than that in CD_3OD. The same spectrum is obtained on dissolution of **3** or **4** in $(CD_3)_2SO$.

Discussion

The ability of the $[Co_4O_4]^{4+}$ core to be protonated indicates that even when bridging three Co^{3+} ions, the μ_3-O^{2-} ions retain significant basicity. This is consistent with the previous observation that these oxide ions of the $[Co_4O_4]^{4+}$ core can also attach to Co^{2+} centers and give $[Co_8O_4(O_2CPh)_{12}(MeCN)_3(H_2O)]$.[8] The first protonation is rather facile, but the second requires strongly acidic conditions, precluding any further protonations.

A search of the structural literature reveals no previous structurally characterized examples of $[M_4O_{4-x}(OH)_x]$ cubane units for $x = 1$, 2, or 3. There are, however, many examples of complexes with a $[M_4(OH)_4]$ cubane core, the vast majority of these being organometallic with formulation $[M_4(OH)_4(CO)_{12}]$ (M = Mn,[15] Re,[15c,16] Cr,[17] Mo,[18] W[19]), $[Mo_4(OH)_4(CO)_8$-

(15) (a) Horn, E.; Snow, M. R.; Zeleney, P. C. *Aust. J. Chem.* **1980**, *33*, 1659. (b) Copp, S. B.; Subramanian, S.; Zaworotko, M. J. *J. Am. Chem. Soc.* **1992**, *114*, 8719. (c) Copp, S. B.; Holman, K. T.; Sangster, J. O. S.; Subramanian, S.; Zaworotko, M. J. *J. Chem. Soc., Dalton Trans.* **1995**, 2233. (d) Clerk, M. D.; Copp, S. B.; Subramanian, S.; Zaworotko, M. J. *Supramol. Chem.* **1992**, *1*, 7.

(16) (a) Nuber, B.; Oberdorfer, F.; Ziegler, M. L. *Acta Crystallogr., Sect. B* **1981**, *37*, 2062. (b) Breimair, J.; Robl, C.; Beck, W. *J. Organomet. Chem.* **1991**, *411*, 395. (c) Copp, S. B.; Subramanian, S.; Zaworotko, M. J. *Angew. Chem., Int. Ed. Engl.* **1993**, *32*, 706.

(17) McNeese, T. J.; Mueller, T. E.; Wierda, D. A.; Darensbourg, D. J.; Delord, T. J. *Inorg. Chem.* **1985**, *24*, 3465.

(18) (a) Marsh, R. E. *Acta Crystallogr., Sect. B* **1995**, *51*, 897. (b) Beyerholm, A.; Brorson, M.; Minelli, M.; Skov, L. K. *Inorg. Chem.* **1992**, *31*, 3672.

(19) (a) Albano, V. G.; Ciani, G.; Manassero, M.; Sansoni, M. *J. Organomet. Chem.* **1972**, *34*, 353. (b) Lin, J. T.; Yeh, S. K.; Lee, G. H.; Wang, Yu. *J. Organomet. Chem.* **1989**, *361*, 89.

$(NO)_4]$,[20] $[Pt_4(OH)_4Me_{12}]$,[21] $[Cd_4(OH)_4(C_6F_5)_4]$,[22] $[Ru_4(OH)_4(C_5Me_5)_4]$,[23] and $[Ru_4(OH)_4(C_6H_6)_4]$,[24] with formal metal oxidation states of M^I or M^{II}, except for the Pt complexes, which are formally Pt^{IV}. Several other complexes, within coordination cluster chemistry, are however more related to those in the present work. These are $[Cu_4(OH)_4(TPA)_4(CF_3SO_3)_2]^{2+}$ (TPA = tris(2-pyridyl)amine),[25] $[Cu_4(OH)_4(bpy)_4]^{4+}$,[26] $[Ni_4(OH)_4(TAC)_4]^{4+}$ (TAC = 1,3,5-triaminocyclohexane),[27] and $[Ni_4(OH)_4(py)_4(TT)_4]$ (TT = 1,3-thiazolidine-2-thionato),[28] all containing M^{2+} ions.

Conclusions

The $[Co_4O_4]^{4+}$ core has been found to be capable of undergoing protonation reactions to yield isolable derivatives. A maximum of two H^+ can be added under the conditions employed to date and with the $[Co_4O_4(O_2CR)_2(bpy)_4]^{2+}$ complexes available. Although no tri- or tetraprotonated derivatives have been obtained, this may be due to charge buildup, and further protonations might prove to be possible with negatively charged complexes such as $[Co_4O_4(O_2CR)_2(L)_4]^{2-}$ (L = an anionic chelate), but these are currently unavailable.

The diprotonated complex is a strong acid, whereas the monoprotonated complex is a weak acid with a pK_a of 3.15, similar to, for example, iodoacetic acid (3.12). In this regard, the diprotonated complex is akin to sulfuric acid. Thus, it would be expected that the monoprotonated species would be the main species in solution, and this is indeed consistent with available spectroscopic data.

The combined results in this and previous work suggest that the $[Co_4O_4]^{4+}$ core should be capable as acting as an inert central kernel on which can possibly be added a variety of Lewis acidic ions, such as the Co^{II} and H^+ ions already employed. Such a route to controlled aggregation of mixed-metal clusters of controllable composition and structure might be useful to possess.

Acknowledgment. This work was supported by the National Science Foundation.

Supporting Information Available: X-ray structural details for complexes **5** and **6**. Two X-ray crystallographic files, in CIF format, are available. This material is available free of charge via the Internet at http://pubs.acs.org.

IC981237N

(20) Albano, V.; Bellon, P.; Ciani, G.; Manassero, M. *J. Chem. Soc. D* **1969**, 1242.
(21) (a) Spiro, T. G.; Templeton, D. H.; Zalkin, A. *Inorg. Chem.* **1968**, *7*, 2165. (b) Preston, H. S.; Mills, J. C.; Kennard, C. H. L. *J. Organomet. Chem.* **1968**, *14*, 447. (c) Cowan, D. O.; Krieghoff, N. G.; Donnay, G. *Acta Crystallogr. Sect. B.* **1968**, *24*, 287.
(22) Weidenbruch, M.; Herrndorf, M.; Schaefer, A.; Pohl, S.; Saak, W. *J. Organomet. Chem.* **1989**, *361*, 139.
(23) Suzuki, H.; Kakigano, T.; Igarashi, M.; Usui, A.; Noda, K.; Oshima, M.; Tanaka, M.; Moro-oka, Y. *Chem. Lett.* **1993**, 1707.
(24) Gould, R. O.; Jones, C. L.; Robertson, D. R.; Tocher, D. A.; Stephenson, T. A. *J. Organomet. Chem.* **1982**, *226*, 199.
(25) Dedert, P. L.; Sorfell, T.; Marks, T. J.; Ibers, J. A. *Inorg. Chem.* **1982**, *21*, 3506.
(26) Sletten, J.; Sorensen, A.; Julve, M.; Journaux, Y. *Inorg. Chem.* **1990**, *29*, 5054.
(27) Aurivillius, B. *Acta Chem. Scand. Ser. A* **1977**, *31*, 501.
(28) Ballester, L.; Coronado, E.; Gutierrez, A.; Monge, A.; Perpinan, M. F.; Pinilla, E.; Rico, T. *Inorg. Chem.* **1992**, *31*, 2053.